Host and parasite thermal ecology jointly determine the effect of climate warming on epidemic dynamics

Alyssa-Lois M. Gehman[a,1,2], Richard J. Hall[a,b,c], and James E. Byers[a,c]

[a]Odum School of Ecology, University of Georgia, Athens, GA 30602; [b]Department of Infectious Diseases, College of Veterinary Medicine, University of Georgia, Athens GA 30602; and [c]Center for the Ecology of Infectious Diseases, University of Georgia, Athens, GA, 30602

Edited by George N. Somero, Stanford University, Pacific Grove, CA, and approved November 28, 2017 (received for review March 27, 2017)

Host–parasite systems have intricately coupled life cycles, but each interactor can respond differently to changes in environmental variables like temperature. Although vital to predicting how parasitism will respond to climate change, thermal responses of both host and parasite in key traits affecting infection dynamics have rarely been quantified. Through temperature-controlled experiments on an ectothermic host–parasite system, we demonstrate an offset in the thermal optima for survival of infected and uninfected hosts and parasite production. We combine experimentally derived thermal performance curves with field data on seasonal host abundance and parasite prevalence to parameterize an epidemiological model and forecast the dynamical responses to plausible future climate-warming scenarios. In warming scenarios within the coastal southeastern United States, the model predicts sharp declines in parasite prevalence, with local parasite extinction occurring with as little as 2 °C warming. The northern portion of the parasite's current range could experience local increases in transmission, but assuming no thermal adaptation of the parasite, we find no evidence that the parasite will expand its range northward under warming. This work exemplifies that some host populations may experience reduced parasitism in a warming world and highlights the need to measure host and parasite thermal performance to predict infection responses to climate change.

disease ecology | thermal performance curves | marine ecology | epidemiological modeling | rhizocephalans

Individuals respond physiologically to environmental change, and these responses can profoundly influence population dynamics and species interactions (1). Quantifying sensitivity to the environment in traits of hosts and their parasites is particularly important because it may alter the spread and transmission of infectious diseases, including those of public health concern. Warming in temperate regions is predicted to increase the distribution and activity of ectothermic vectors of human pathogens, which, coupled with an increase in vector and parasite development rates, might result in higher transmission potential (2, 3). Alternatively, for regions where high temperatures cause vectors to suffer higher mortality rates (4), warming could reduce transmission potential (5). Further, recent niche modeling suggests that climate change could lead many parasite species to extinction (6). A mechanistic understanding of how environmental change will influence hosts and their parasites is vital for predicting infection outcomes (7, 8).

To evaluate temperature effects on species interactions requires integrating across multiple organismal responses (4). Temperature can differentially influence parasite and host performance processes, such as reproduction and survival, complicating predictions of the net effect of warming on species interactions (9). For example, greater parasite reproduction with temperature may not change parasite dynamics if increased temperature also enhances parasite-induced mortality within the host (10). Empirical data are limited, even in human disease systems, with physiological response estimates often combined from multiple species, or from spatially distinct regions (2, 4). A comprehensive analysis of the effects of temperature on multiple stages of infection within a single host–parasite system has not yet been accomplished.

Ectothermic host–parasite interactions provide tractable systems to evaluate temperature effects on species interactions. Ectotherms are dependent on external sources of heat, and environmental temperature is one of the most important factors affecting their performance, with many physiological and behavioral attributes sensitive to temperature (11, 12). Differences in thermal performance optima and thresholds of physiological responses between host and parasite could lead to altered outcomes of their interactions as thermal regimes shift. In particular, parasites could place physiological demands on their hosts that alter host thermal performance relative to uninfected individuals, which could impact how key transmission processes respond to increased temperature. Empirical evidence to explore temperature effects on hosts and parasites is crucially needed to predict population dynamic responses to warming (7, 8).

We test the prediction that parasite and host traits have different thermal performance curves and quantitatively evaluate how differences in thermal performance affect predictions of climate warming on disease dynamics. We focus on an ectothermic host–parasite system that exhibits pronounced seasonal variation in infection prevalence (13) and whose biogeographic spread might be limited by high summer temperatures (14). *Eurypanopeus depressus* is an abundant oyster reef-dwelling crab that is infected with a nonnative rhizocephalan parasite, *Loxothylacus panopaei*. As an ectotherm, *E. depressus* body temperature can be expected to conform to the surrounding water temperature. Parasites are transmitted via production of a short-lived free-living stage that recruits to uninfected hosts (detailed lifecycle in *SI Appendix*, *Materials and Methods* and Fig. S1). There are two distinct stages of *L. panopaei* infection: exposed

Significance

Experiments and modeling demonstrate that vital rates of a host and parasite respond differently to temperature, with local parasite extinction in the coastal southeastern United States predicted under climate warming. Quantifying and comparing thermal performance curves for multiple host and parasite traits can help identify locations and temperature regimes in which parasitism could decrease or increase under future warming, depending on the temperature difference between host and parasite performance optima. We suggest that such comparative work might resolve conflicting predictions of whether hosts or parasites have the upper hand in a warming world.

Author contributions: A.-L.M.G., R.J.H., and J.E.B. designed research; A.-L.M.G. and R.J.H. performed research; A.-L.M.G. and R.J.H. analyzed data; and A.-L.M.G., R.J.H., and J.E.B. wrote the paper.

The authors declare no conflict of interest.

This article is a PNAS Direct Submission.

Published under the PNAS license.

Data deposition: R code and data related to this manuscript have been deposited at https://github.com/alyssamina/Thermal-ecology-disease.

[1]To whom correspondence should be addressed. Email: alyssamina@gmail.com.

[2]Present address: Department of Zoology, University of British Columbia, Vancouver, BC V6T 1Z4, Canada.

This article contains supporting information online at www.pnas.org/lookup/suppl/doi:10.1073/pnas.1705067115/-/DCSupplemental.

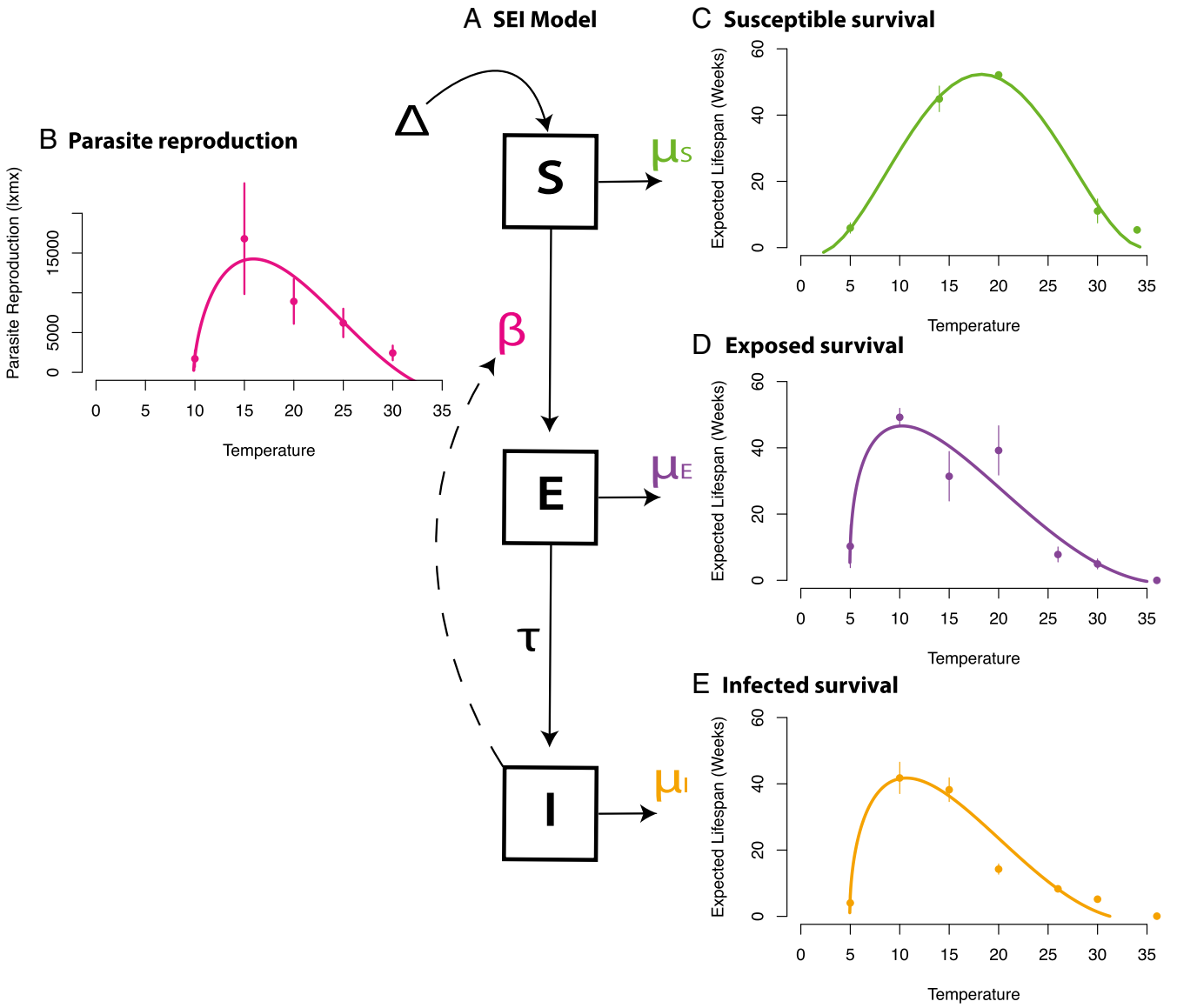

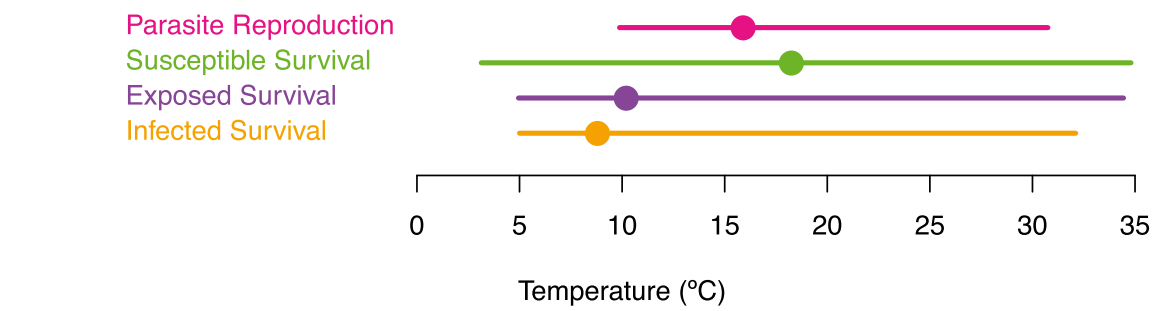

Fig. 1. (*A*) A model schematic for *L. panopaei* transmission in *E. depressus*. Susceptible hosts, S, are recruited at a constant weekly rate, Δ, during the recruitment period (of duration, *d*, and timing, *p*; details in *SI Appendix, Materials and Methods*) and die at per capita rate μ_s (= 1/expected lifespan). Susceptible hosts become parasitized at per capita rate βSI, where the transmission rate, β, is an agglomerate parameter assumed proportional to larval parasite production, $P(T)$ (*SI Appendix, Materials and Methods*), and *I* is the number of infectious hosts with the reproductively mature parasite stage. Exposed hosts, *E*, are infected with reproductively immature parasites that develop at rate τ. Exposed and infectious hosts have respective mortality rates μ_E and μ_I. Model parameters labeled in color are temperature-dependent and are parameterized based on thermal performance curves fit to experimental measurements of (*B*) parasite reproduction (lifetime reproduction, lxmx) and host survival for each infection status: (*C*) susceptible, (*D*) exposed, and (*E*) infected (*SI Appendix, Materials and Methods*). (*F*) Thermal performance range (lines) and optima (points) for susceptible, exposed, and infected survival and parasite reproduction calculated from controlled laboratory experiments (*B*–*E*).

hosts, which are infected with nonreproductive parasite stages that develop internally, and infected hosts, in which the parasite is reproductive and releasing infective stages (*SI Appendix*, Fig. S1 *E* and *H*, respectively). In Savannah, Georgia, toward the southern end of the host's and parasite's range (*SI Appendix*, Fig. S16), we conducted laboratory experiments in which we subjected uninfected hosts (susceptible) and the two stages of parasite-infected hosts (exposed and infected) to temperature treatments encompassing the annual temperature range of coastal Georgia (*SI Appendix*, *Materials and Methods*). These were used to parameterize thermal performance curves for expected host lifespan by infection status and parasite production, yielding estimates of the thermal optima (T_{opt}) and the thermal range (thermal minimum = T_{min}; thermal maximum = T_{max}) for which the trait exceeded zero.

Survival of susceptible hosts was nonlinearly related to temperature, with $T_{min} = 3.14$ °C, $T_{max} = 34.80$ °C, and $T_{opt} \approx 18.26$ °C (Fig. 1 *C* and *F* and *SI Appendix*, Table S2). Parasitized hosts had a substantially lower T_{opt} for survival, whether the parasite was actively reproductive or not (infected $T_{opt} = 8.83$ °C and exposed $T_{opt} = 10.24$ °C; Fig. 1 *D*–*F* and *SI Appendix*, Table S2). Hosts with active parasite reproduction (infected) had a lower lethal maximum temperature than uninfected crabs ($T_{max} = 32.10$ °C; Fig. 1 *E* and *F*). Parasite reproduction was optimized at temperatures closer to the optimal survival temperature of uninfected than infected hosts ($T_{opt} \approx 15.90$ °C) and had a more restricted thermal range ($T_{min} = 9.88$ °C and $T_{max} = 30.75$ °C; Fig. 1 *B* and *F* and *SI Appendix*, Table S2). Together, the parasitized hosts had optimal performance at lower temperatures than that of the uninfected hosts. The offset in T_{opt} of 8–10 °C between uninfected and infected host survival reveals that parasite infection can drive a sizable change in host thermal performance, thus causing a mismatch in the thermal performance optima and breadth of the vital rates of parasite versus host (Fig. 1).

We investigated the ecological consequences of seasonal mismatch in thermal performance for host and parasite by developing a compartmental model of host infection (15), where parasite transmission and host survival are temperature-dependent (Fig. 1). The model describes local disease dynamics in an *E. depressus* population on an oyster reef within an estuary and therefore assumes open host recruitment and closed parasite recruitment (*SI Appendix*, *Materials and Methods* and ref. 16). Thermal performance curves (Fig. 1) were used to parameterize how host mortality and parasite production depended on weekly mean temperatures. To describe the thermal environment of the host and parasite we calculated mean weekly temperatures from a mooring that is part of the Georgia Coastal Ecosystems Long Term Ecological Research program (GCE-LTER) that measured temperature at a depth of ∼1 m, the approximate depth of water found over an oyster reef in Georgia (17–21), and thus the thermal environment experienced by *E. depressus* and *L. panopaei*.

Temperature is also likely to influence the performance of free-living larval stages of the host and parasite (i.e., decrease survivorship and alter infectivity), as well as the internal development rate of parasites within hosts; however, we did not measure larval performance in our experiment, and a lack of published estimates on how rhizocephalan larvae respond to temperature means that we have no information on thermal performance of these stages in our system. Consequently, we assumed that the parasite development rate (τ), life span ($1/\mu_W$), infectivity (λ_f), and the weekly host recruitment rate (Δ), together with its seasonal duration (d) and timing (p), were constant. This means that infection dynamics are likely to be even more sensitive to temperature than our model predicts. In particular, our model likely overestimates the true temperature range for which transmission is possible, making our results conservative. The weekly host recruitment rate was estimated from the literature (22), and the remaining four parameters (d, p, b, and τ) were chosen to give good quantitative agreement between model output and field data on seasonal host infection prevalence and subject to extensive sensitivity analyses (*SI Appendix*, *Materials and Methods*).

The model dynamics rapidly converge on an annually repeating seasonal cycle of infection prevalence (*SI Appendix*, Fig. S10), characterized by an increase in the winter and early spring and followed by a decrease in late spring and early summer (Fig. 2*A*). Peak prevalence is coincident with decreasing susceptible and exposed populations and rising infected populations (Fig. 2). The decrease in prevalence in the summer is driven by a combination of decreased parasite transmission (*SI Appendix*, Fig. S6*C*) and greater infected host mortality (*SI Appendix*, Fig. S6*E*) with the seasonal increase in temperature (*SI Appendix*, Fig. S6*A*). The maintenance of low infection prevalence over several months in the fall is due in large part to an influx of new host recruits to the susceptible class (Fig. 2). Qualitatively, our fitted model is able to recapture the seasonal pattern of field measurements of infection prevalence that increase in the spring and decrease sharply in the early summer, correlated with temperatures reaching above 25 °C (13). Since the parasite is castrating, we ran a variant of the model where the decoupled, external recruitment of hosts was instead reduced proportional to infection prevalence, assuming that all reefs within an estuary experience similar epidemics (*SI Appendix*,

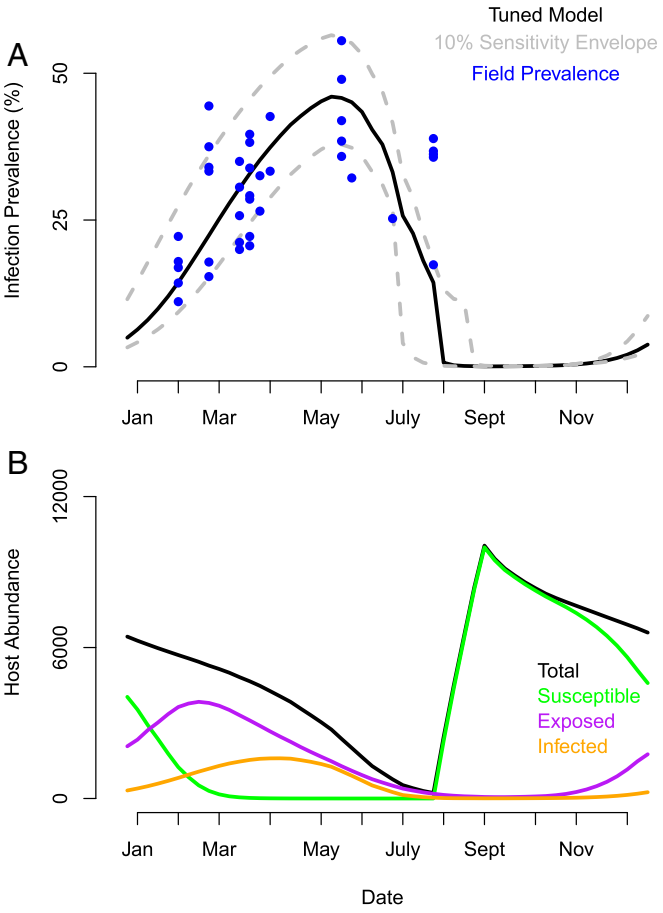

Fig. 2. (*A*) Epidemiological model output predicting seasonal changes in *L. panopaei* infection prevalence in *E. depressus* (black line) based on temperature-dependent parameters [μ_S, μ_E, μ_I, and $\beta = bP(T)$; Fig. 1] updated weekly using historic mean weekly temperatures from 2011 to 2014 at the GCE-LTER mooring (Fig. 3*A*). Model parameters not measured or estimable from published literature (p, d, b, and τ; *SI Appendix*, *Materials and Methods*) were tuned to match peak infection prevalence and its timing (*SI Appendix*, *Materials and Methods*); the sensitivity of model output to the parameterization is illustrated as the envelope of maximum and minimum prevalence when all tuned parameters are covaried by ±10% (gray dashed lines). The model prediction of seasonal infection prevalence is overlaid above empirical measurements of *L. panopaei* prevalence from Romerly Marsh, Savannah, Georgia, from 2010 to 2014 (blue dot). (*B*) Model output of susceptible (green), exposed (purple), infected (orange), and total host abundance (black) for an average reef in Savannah, Georgia, through the annual cycle (*SI Appendix*, *Materials and Methods*).

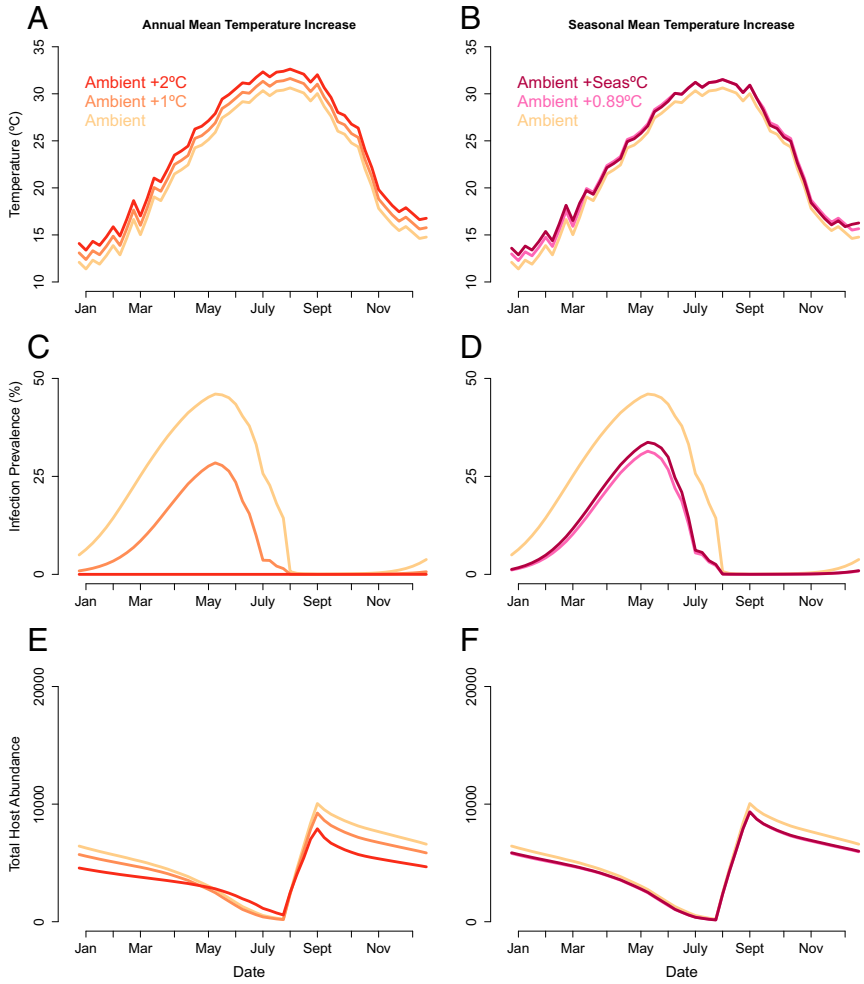

Fig. 3. (*A*) Temperatures used to drive seasonality in the host–parasite model, with the mean weekly water temperature from the GCE-LTER mooring averaged weekly from 2011 to 2014 (ambient; peach) and two warming scenarios, ambient +1 °C (orange) and ambient +2 °C (red). (*B*) Ambient temperature (peach) and temperature increase based on actual measured historical temperature change in the southeast from 1970 to 2008 (24), with the measured increase of ambient +0.89 °C applied uniformly throughout the year (pink) and with a more realistic increase that averaged +0.89 °C but varied across seasons; winter = ambient +1.5 °C, spring = ambient +0.67 °C, summer = ambient +0.89 °C, and fall = ambient +0.61 °C (ambient + Seas °C, where Seas indicates seasonal intraannual temperature variation applied; purple). (*C*–*F*) Model outputs across all temperature scenarios for infection prevalence (*C* and *D*) and total host abundance (*E* and *F*).

Materials and Methods). This resulted in lower host abundance and infection prevalence, but no difference in the seasonal pattern of infection (*SI Appendix*, Fig. S12).

To evaluate how robust the prediction of seasonality in prevalence was to the choice of the four parameters fit to the field prevalence data (duration and timing of host recruitment, parasite development rate, and colonization probability), we conducted both qualitative and quantitative sensitivity analyses (*SI Appendix*, *Materials and Methods*). Independently varying and covarying the fitted parameters over biologically plausible ranges maintained the qualitative pattern of a single peak in prevalence in the spring or summer (Fig. 2 and *SI Appendix*, Figs. S7 and S8). Peak and mean prevalence, but not minimum prevalence, increased with parasite colonization probability (b; *SI Appendix*, Fig. S9*B*) and only weakly depended on the seasonal pattern of host recruitment, p and d (*SI Appendix*, Fig. S9*A*) and parasite development rate, τ (*SI Appendix*, Fig. S8*F*). The timing of the seasonal peak in prevalence was most strongly influenced by the combination of timing and duration of host recruitment (*SI Appendix*, Fig. S8*B*). We quantified the relative sensitivity of peak prevalence to these parameters by independently varying them around their fitted values and recording the range over which the timing and magnitude of peak prevalence remained close to those of the best-fit model (i.e., within ±20% peak prevalence and timing of peak prevalence between weeks 17 and 25). Peak prevalence and its timing were relatively insensitive to variations in the timing of host recruitment (from −66 to +130% of its fitted value) and parasite colonization (from −50 to +140%) and somewhat more sensitive to variations in the duration of recruitment (from −25 to +30%) and parasite development rate (from −16 to +4%; *SI Appendix*, Table S4). Together, these sensitivity analyses support our assumption that our experimentally measured thermal performance traits drive the observed seasonal patterns in infection prevalence and therefore that relaxing our simplifying assumptions of temperature-independent host recruitment, parasite internal development, and colonization would be unlikely to change the qualitative patterns in model output.

To evaluate potential effects of climate change on host–parasite interactions in ectothermic hosts within coastal Georgia, we ran the model for two scenarios where the seasonal GCE ambient temperature was raised by a fixed amount of +1 and +2 °C (23). After initial transient dynamics, the model settled into an annually repeating cycle. Seasonal peaks in parasite prevalence within an oyster reef persisted with reduced amplitude under the ambient +1 °C warming scenario, but the parasite was locally extirpated at ambient +2 °C (Fig. 3*C*). Mechanistically, parasite extirpation is driven by a warming-induced increase in infected host mortality

(*SI Appendix*, Fig. S6*E*) and concomitant decrease in parasite transmission (*SI Appendix*, Fig. S6*C*). If parasite castration limits local host recruitment, warming is more likely to lead to parasite extirpation (i.e., parasite extinction occurred after 1 °C warming, *SI Appendix*, *Materials and Methods* and Fig. S12). Combining temperature-dependent traits and seasonal host abundance into an expression for the weekly effective reproductive number of the parasite (*SI Appendix*, *Materials and Methods*) revealed that parasite invasion potential peaks in late fall and winter following the fall host recruitment pulse and drops below the threshold value of one in the summer months (*SI Appendix*, Fig. S14). To synthesize the combined effects of temperature on parasite transmission potential independent of seasonal host recruitment, we derived an expression for the temperature-dependent components of the parasite basic reproductive number, R_0 (*SI Appendix*, *Materials and Methods* and Eq. **S19**). This expression shows a similar right-skewed response to temperature as do the measured experimental parameters (exposed and infected host survival and parasite production; Fig. 1 *B*, *D*, and *E* and *SI Appendix*, Fig. S13).

In the southeastern United States, the increase in temperature as a result of climate change is more pronounced in winter months (24), and this uneven seasonal increase is expected to persist into the future (23). Thus, to explore the effects of a more realistic, seasonally varying temperature change, we applied the actual historical change in temperature in the southeast from 1970 to 2008 (24). We used the change over this time period as the expected temperature increase going forward and modeled the effects of this empirically measured, seasonally variable temperature change (winter = ambient +1.5 °C, spring = ambient +0.67 °C, summer = ambient +0.89 °C, and fall = ambient +0.61 °C; Fig. 3*B*), as well as the mean annual temperature change applied uniformly across the year (ambient +0.89 °C; Fig. 3*B*) over the same time period on host–parasite dynamics (24). The seasonally dependent temperature-change model predicted slightly higher maximum infection prevalence (33.7%) than the mean temperature-change model (31.4%). However, maximum prevalence under both warming scenarios was lower than under present-day (ambient) temperatures (Fig. 3*D*). The slightly higher infection prevalence predicted by the seasonally dependent temperature change is likely driven by the winter increase in temperature. During the winter months, ambient temperatures can be below the reproduction thermal optima of the parasite, so that an increase in temperature in winter has a positive effect on parasite reproduction (*SI Appendix*, Fig. S6*D*).

To investigate the effect of current and future temperatures on parasite dynamics and persistence in the coastal southeastern United States, we repeated our analyses using temperature data from sites ∼150 km to the north (Ace Basin, South Carolina) and south (St. Augustine, Florida) of our study site (Table S5; data from the National Estuarine Research Reserve System, cdmo.baruch.sc.edu/). At all sites, the model predicts that infection prevalence will decline under both 1° and 2 °C warming scenarios (Fig. 4). At the southern site, current and future warming prevalence was always lower than in Georgia, with parasite extinction occurring with 2 °C warming, suggesting that climate warming threatens the parasite throughout the southern edge of its range. However, at the South Carolina site, current infection prevalence was higher, and simulated temperature increases resulted in less dramatic prevalence declines than in Georgia; notably, the parasite persisted under the 2 °C warming scenario. Our model results corroborate regional-scale observations that suggest that the parasite is thermally limited at its southern range edge (14).

Because crabs at more distant locales may experience different abiotic conditions (e.g., salinity; ref. 25) or biotic conditions (e.g., predation rates; ref. 26) that could influence seasonal recruitment patterns and local thermal performance relative to those experienced in Georgia, we restricted full-model predictions to the southern part of the parasite's current range. However, the parasite has recently expanded its northern range to Long Island Sound, New York, in part due to human-mediated dispersal (27). Furthermore, the sharp increase in the temperature-dependent R_0 curve above the lower thermal limit for parasite reproduction (*SI Appendix*, Fig. S13) suggests high sensitivity to increases in minimum temperatures and thus potential for cool-season parasite transmission to increase under warming at more northerly latitudes.

To explore whether warming might result in local increases in parasite transmission and northward expansion of the parasite's current range, we selected seven locations spanning the host's range along the Atlantic coast, including one site north of the parasite's current known range, and investigated how 1 and 2 °C increases to current mean weekly temperatures would change the number of weeks conducive to parasite transmission (*SI Appendix*, *Materials and Methods*). At the current northern range edge we found no evidence that warming will drive a northern range expansion because mean winter temperatures remain too low to support parasite reproduction, and the number of weeks above optimal transmission temperatures in summer increases (*SI Appendix*, Fig. S16). However, at latitudes between 34 and 40°, we found that increases in cool season temperatures result in a net increase in the number of weeks conducive to transmission (*SI Appendix*, Fig. S16). Together, these suggest that warming could result in a net range contraction, primarily due to extirpation in the south, but that local increases in transmission could occur in the northern part of the current range. We stress, however, that these predictions assume no local thermal adaptation by the host or parasite, and thus recommend additional efforts to quantify host and parasite thermal performance in the northern portion of the range to more accurately predict how seasonal prevalence patterns will change under warming.

This work highlights the consequences of mismatches in host and parasite thermal performance for parasite persistence. Our experiments reveal that parasite infection influences host thermal performance by disproportionately reducing infected host survival at higher temperatures (Fig. 1*E*). The ensuing difference in the temperatures that optimize uninfected and infected host survival results in decreased infection prevalence and even local parasite extirpation under projected warming in the coastal southeastern United States (Fig. 3*C*). While physiological theory predicts that many traits should increase gradually with temperature to the thermal optimum and then decrease rapidly (i.e., they are left-skewed; refs. 28 and 29), we find evidence of the opposite pattern for parasite production and infected host survival (Fig. 1 *B*, *D*, and *E*). Right skews in thermal performance have been shown in individual ectothermic organisms (30), but have rarely been investigated in host–parasite pairs. For parasites that can reproduce facultatively off of their hosts (e.g., *Batrachochytrium dendrobatidis*), it has been suggested that a

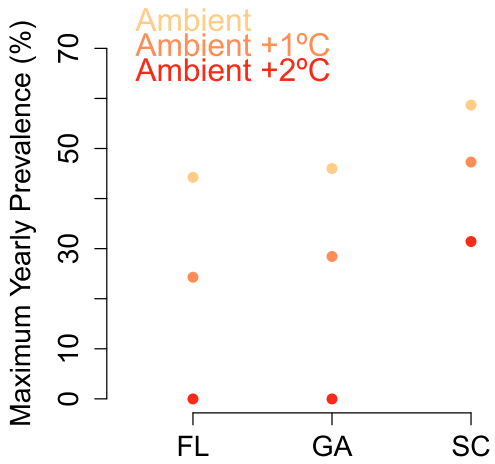

Fig. 4. Maximum yearly prevalence (%) predicted from model outputs run with weekly water temperature data from 2011 to 2014 for St. Augustine, Florida (FL); a GCE-LTER mooring, Georgia (GA); and Ace Basin, South Carolina (SC). We ran the model with ambient conditions (peach) and two warming scenarios, ambient +1 °C (orange) and ambient +2 °C (red).

right-skewed performance curve can result when parasite off-host growth outperforms host growth at temperatures lower than host and parasite thermal optima (31). However, because many parasites, including *L. panopaei*, obligately require their hosts to grow and reproduce, this mechanism cannot explain right skews for all systems. In our system, uninfected host survival was optimized at a temperature close to that which optimizes parasite reproduction, whereas infected host survival was optimized just below the parasite reproductive thermal minimum (Fig. 1*F*). This suggests that costs associated with the onset of parasite reproduction could be driving the decrease in infected host survival at temperatures close to those that optimize uninfected host survival.

Our study suggests that predicting more generally how host–parasite systems will respond to climate warming may depend crucially on both host and parasite thermal performance and differences in host performance driven by parasite infection. Temperature is known to influence pathogen-infected host performance in terrestrial plants and insects (32, 33) and may also influence endothermic host behavior in ways that alter their exposure risk to pathogens (34, 35). Because host abundance and infectious period are key components of pathogen fitness, as summarized by the parasite basic reproductive number, R_0 (*SI Appendix*, Eq. **S18**), omitting temperature dependence in associated uninfected and infected host traits could lead to incorrect predictions about the magnitude and direction of changes in infection prevalence under warming.

Inclusion of nonlinear effects of temperature on parasites, as was done in this study, will likely increase the accuracy of predictions of host–parasite interactions at higher temperatures (4) and will be particularly important in light of the fact that temperature changes have not been equal between seasons and are not expected to be equal in the future (24). Indeed, our model results can be used to evaluate the potential effects of increased variability in temperature extremes and suggests that warmer winters could ameliorate the negative effects of climate change on this parasite, but that warmer summer temperatures could do the opposite (Fig. 3*D*).

In sum, this work reveals a thermal offset in performance between uninfected and infected hosts that leads to the prediction of local declines or even local extirpation of the parasite under modest climate-warming scenarios. In addition, the same framework highlights areas within the parasite's range where temperature change could increase infection. We propose that the extent of offset between host and parasite performance in response to temperature or other environmental gradients could be an important general predictor for how host–parasite pairs will respond to future environmental change and could help explain the variability in host–parasite responses to warming that has created the wealth of debate on the topic.

ACKNOWLEDGMENTS. We thank A. Penn, S. Perry, S. Bourget, R. Smith, S. Sims, M. Holden, K. Davis, R. Usher, C. Madden, and staff at the Skidaway Institute of Oceanography for field and laboratory assistance. We thank the J.E.B., Osenberg, and Harley laboratories for discussion and J. Porter, S. Altizer, V. Ezenwa, W. Fitt, T. Dallas, and two anonymous reviewers for manuscript feedback. Support came from the M.K. Pentecost Ecology Fund and the Odum School of Ecology. A.-L.M.G. was a Wormsloe Institute for Environmental History Fellow.

1. Doney SC, et al. (2012) Climate change impacts on marine ecosystems. *Annu Rev Mar Sci* 4:11–37.
2. LaDeau SL, Allan BF, Leisnham PT, Levy MZ (2015) The ecological foundations of transmission potential and vector-borne disease in urban landscapes. *Funct Ecol* 29: 889–901.
3. Ren Z, et al. (2016) Predicting malaria vector distribution under climate change scenarios in China: Challenges for malaria elimination. *Sci Rep* 6:20604.
4. Mordecai EA, et al. (2013) Optimal temperature for malaria transmission is dramatically lower than previously predicted. *Ecol Lett* 16:22–30.
5. Ryan SJ, et al. (2015) Mapping physiological suitability limits for malaria in Africa under climate change. *Vector Borne Zoonotic Dis* 15:718–725.
6. Carlson CJ, et al. (2017) Parasite biodiversity faces extinction and redistribution in a changing climate. *Sci Adv* 3:e1602422.
7. Altizer S, Ostfeld RS, Johnson PTJ, Kutz S, Harvell CD (2013) Climate change and infectious diseases: From evidence to a predictive framework. *Science* 341:514–519.
8. Rohr JR, et al. (2011) Frontiers in climate change-disease research. *Trends Ecol Evol* 26: 270–277.
9. Lafferty KD, Holt RD (2003) How should environmental stress affect the population dynamics of disease? *Ecol Lett* 6:654–664.
10. Anderson RM, May RM (1979) Prevalence of schistosome infections within molluscan populations: Observed patterns and theoretical predictions. *Parasitology* 79:63–94.
11. Dell AI, Pawar S, Savage VM (2011) Systematic variation in the temperature dependence of physiological and ecological traits. *Proc Natl Acad Sci USA* 108: 10591–10596.
12. Amarasekare P, Sifuentes R (2012) Elucidating the temperature response of survivorship in insects. *Funct Ecol* 26:959–968.
13. O'Shaughnessy KA, Harding JM, Burge EJ (2014) Ecological effects of the invasive parasite *Loxothylacus panopaei* on the flatback mud crab *Eurypanopeus depressus* with implications for estuarine communities. *Bull Mar Sci* 90:611–621.
14. Kruse HH, Hare MP, Hines AH (2011) Genetic relationships of the marine invasive crab parasite *Loxothylacus panopaei*: An analysis of DNA sequence variation, host specificity, and distributional range. *Biol Invasions* 14:701–715.
15. Anderson RM, May RM (1982) Coevolution of hosts and parasites. *Parasitology* 85: 411–426.
16. Kuris AM, Lafferty KD (1992) Modelling crustacean fisheries: Effects of parasites on management strategies. *Can J Fish Aquat Sci* 49:327–336.
17. Byers JE, et al. (2015) Geographic variation in intertidal oyster reef properties and the influence of tidal prism. *Limnol Oceanogr* 60:1051–1063.
18. Di Iorio D (2012) Data from "Continuous salinity, temperature and depth measurements from moored hydrographic data loggers deployed at GCE10_Hydro (Duplin River west of Sapelo Island, Georgia) from 01-Jan-2011 through 31-Dec-2011." 10.6073/pasta/c705a3cf1492716c7ac19d7cd1423b55.
19. Di Iorio D (2013) Data from "Continuous salinity, temperature and depth measurements from moored hydrographic data loggers deployed at GCE10_Hydro (Duplin River west of Sapelo Island, Georgia) from 01-Jan-2012 through 31-Dec-2012." 10.6073/pasta/73b48d6008a86509291b97e513307b85.
20. Di Iorio D (2014) Data from "Continuous salinity, temperature and depth measurements from moored hydrographic data loggers deployed at GCE10_Hydro (Duplin River west of Sapelo Island, Georgia) from 01-Jan-2013 through 31-Dec-2013." 10.6073/pasta/9f24a43f1d02b3f80c9cff2dfc9e33e5.
21. Di Iorio D (2014) Data from "Continuous salinity, temperature and depth measurements from moored hydrographic data loggers deployed at GCE10_Hydro (Duplin River west of Sapelo Island, Georgia) from 01-Jan-2014 through 31-Dec-2014", 10.6073/pasta/1b0236a552de365151163eb530299469.
22. Gehman AM, et al. (2017) Predators, environment and host characteristics influence the probability of infection by an invasive castrating parasite. *Oecologia* 183:139–149.
23. Christensen JH, et al. (2007) 2007: Regional climate projections. *Climate Change 2007: The Physical Science Basis. Contribution of Working Group 1 to the Fourth Assessment of the Intergovernmental Panel on Climate Change* (Cambridge Univ Press, New York), Chap 11.
24. Karl T, Melillo J, Peterson T (2009) *Global Climate Change Impacts in the United States* (Cambridge Univ Press, New York).
25. Reisser C, Forward R, Jr (1991) Effect of salinity on osmoregulation and survival of a rhizocephalan parasite, *Loxothylacus panopaei*, and its crab host, *Rhithropanopeus harrisii*. *Estuaries Coasts* 14:102–106.
26. Gehman AM, Byers JE (2017) Non-native parasite enhances susceptibility of host to native predators. *Oecologia* 183:919–926.
27. Freeman AS, Blakeslee AMH, Fowler AE (2013) Northward expansion of the rhizocephalan *Loxothylacus panopaei* (Gissler, 1884) in the northwest Atlantic. *Aquat Invasions* 8:347–353.
28. Deutsch CA, et al. (2008) Impacts of climate warming on terrestrial ectotherms across latitude. *Proc Natl Acad Sci USA* 105:6668–6672.
29. Huey RB, Stevenson RD (1979) Integrating thermal physiology and ecology of ectotherms: A discussion of approaches. *Am Zool* 19:357–366.
30. San Choi K, Kim D-S (2016) Effect of temperature on the fecundity and longevity of *Ascotis selenaria* (Lepidoptera: Geometridae): Developing an oviposition model. *J Econ Entomol* 109:1267–1272.
31. Cohen JM, et al. (2017) The thermal mismatch hypothesis explains host susceptibility to an emerging infectious disease. *Ecol Lett* 20:184–193.
32. Thomas MB, Blanford S (2003) Thermal biology in insect-parasite interactions. *Trends Ecol Evol* 18:344–350.
33. Pandey P, Ramegowda V, Senthil-Kumar M (2015) Shared and unique responses of plants to multiple individual stresses and stress combinations: Physiological and molecular mechanisms. *Front Plant Sci* 6:723.
34. Small C, Cohen JE (2004) Continental physiography, climate, and the global distribution of human population. *Curr Anthropol* 45:269–277.
35. Saino N, et al. (2007) Temperature and rainfall anomalies in Africa predict timing of spring migration in trans-Saharan migratory birds. *Clim Res* 35:123–134.